Investigating Electrical Drive Performance Employing Model Predictive Control and Active Disturbance Rejection Control Algorithms

Ahmed Aboelhassan, Ahmed M. Diab, Michael Galea, Serhiy Bozhko

University of Nottingham
UK | CHINA | MALAYSIA

University of Nottingham Ningbo China, 199 Taikang East Road, Ningbo, 315100, China

First published 2020

University of Nottingham
UK | CHINA | MALAYSIA

Investigating Electrical Drive Performance Employing Model Predictive Control and Active Disturbance Rejection Control Algorithms

Ahmed Aboelhassan, Ahmed M. Diab, Michael Galea, Serhiy Bozhko
Key Laboratory of More Electric Aircraft Technology of Zhejiang Province, University of Nottingham, Ningbo, China.

***Abstract*-- Many issues can degrade the electrical drive performance such as cross-coupling, time delay, external disturbances, and parameter variation. The Synchronous Reference Frame (SRF) PI Current Controller (CC) is the most popular control scheme for the motor drive current control due to its simplicity. However, the PI controller does not have an optimal dynamic response due to the reasonably low transient response of the integral parts. Furthermore, the tuning of the PI controller depends heavily on the machine's parameters. Recently, alternative control schemes such as Model Predictive Control (MPC) and Active Disturbance Rejection Control (ADRC) are studied due to their dynamic performance and disturbance rejection capability, respectively. This paper presents a comparative study between the conventional PI, ADRC, and MPC control schemes applied for Permanent Magnet Synchronous Motor (PMSM) taking into consideration the operational issues of electrical drives.**

Index Terms — **Active Disturbance Rejection Control, Current Control, Electrical Motor Drive, Model Predictive Control.**

I. INTRODUCTION

The Permanent Magnet Synchronous Motor (PMSM) is widely used in different applications due to its high efficiency, power density, and even increasing reliability features [1-3]. However, some challenges affect the overall performance of the PMSM drive system. For example, the cross-coupling between the orthogonal current components is represented as a nonlinear term and affects the controller behavior [4, 5]. Also, the time delay due to the inverter or the digital computations in the controller limits the control system bandwidth and affects its stability [6]. An external disturbance could occur, for example, due to a sudden impact of the mechanical loads. The machine parameters could be changed according to the operating conditions or different loading behavior [7, 8].

In terms of control schemes, Field Oriented Control (FOC) is considered as the most established strategy for electric drive systems. It consists of cascaded control loops, typically with an inner loop for current regulation and an outer loop for speed control. The most conventional control strategy applied for the current and speed regulation is based on the Proportional-Integral (PI) controller due to its inherent simplicity at design and implementation. It has been applied as a current controller in the Synchronous Reference Frame (SRF) with different configurations to enhance the cross-coupling compensation. However, the tuning of PI gains requires accurate machine parameters to guarantee the desired dynamic performance. Besides, the system bandwidth is limited due to the computational and modulation delay.

Great attention has been given recently to advanced control techniques such as Model Predictive Control (MPC) and Active Disturbance Rejection Control (ADRC) to overcome the stated problems and to enhance the driver dynamic performance. MPC provides higher bandwidth operation compared to the conventional PI controller scheme. It has been implemented as a current controller in [9, 10] showing faster dynamics with lower total harmonic distortion of the motor currents. On the other hand, the ADRC scheme provides high robustness to the internal and external disturbances due to the unmodeled dynamics and parameter uncertainties. It has a great interest in many industrial applications, e.g. flywheel energy storage system [11], DC-DC converters [12, 13], and recently in motor drive systems for current and speed regulations [14-16].

Therefore, in this paper, MPC and ADRC will be applied for PMSM in addition to the common PI control and results will be investigated to compare their dynamic response and their rejection capability for the external and internal disturbances. The rest of the paper is organized as follows: Section II is devoted to the PI control scheme followed by the ADRC algorithm in Section III. MPC and its equations are illustrated in Section IV. The simulation results are mentioned in Section V, while the conclusion is presented in Section VI.

II. THE CONVENTIONAL PI CONTROL SCHEME

Cascaded PI controllers have been implemented for the current and speed regulation as shown in Fig. 1. For the current regulation, two main configurations of the SRF PI CC have been addressed in the literature. The first configuration is known by the conventional SRF PI CC shown in Fig. 2, where $G_p(s)$ represents the machine model and it is illustrated in (1). $G_d(s)$ refers to the computational and modulation delay [17, 18]. It consists of the classical

This work was supported by the Natural Science Foundation of China, through the project with code 51850410515.

PI controller with added feedforward terms to compensate for the cross-couplings effects [19]. The second configuration is the complex vector SRF PI CC. It considers the cross-coupling as a part of the tuning process to achieve pole-zero cancelation resulting in improved dynamic performance and reduction in the machine parameters dependency [20, 21]. It provides better cross-coupling compensation than the conventional scheme[22]. So, the complex vector SRF PI CC has been addressed in this work. The complex SRF PI CC based on the complex vector representation of the AC machine is illustrated in (1) where ω_e is the electrical angular velocity, L and R_s represent the machine inductance and resistance, respectively:

$$G_p(s) = \frac{I_{dq}}{U_{dq}} = \frac{1}{Ls + R_s + j\omega_e L} \quad (1)$$

$$G_{o.l}(s) = \frac{\hat{K}_p s + K_i}{s} \frac{G_d(s)}{Ls + R_s + j\omega_e L}$$

$$= \frac{K_p s + K_i + j\omega_e K_p}{s} \frac{G_d(s)}{Ls + R_s + j\omega_e L} \quad (2)$$

Accordingly, the PI CC can be designed to place the added controller zero on the pole of the plant, as shown by (2). As a result, the controller's zero will be complex, so it is called a "complex current controller". Based on (2), this CC scheme can be structured for the current control loop as shown in Fig. 3. The pole-zero cancelation can be achieved by tuning the controller gains such as:

$$K_i = K_o R_s \quad (3)$$

$$K_p = K_o L \quad (4)$$

The controller gain K_o can be tuned using the root locus of (5) as explained in [20]. From Fig. 1, if the machine parameters used in the tuning process are assumed to match the actual values, the open-loop and closed-loop transfer functions can be expressed as follows:

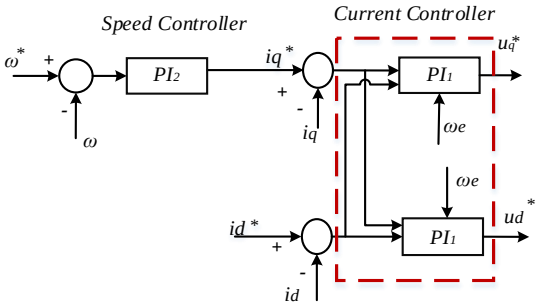

Fig. 1. Block diagram of the cascaded PI controller for the AC machine.

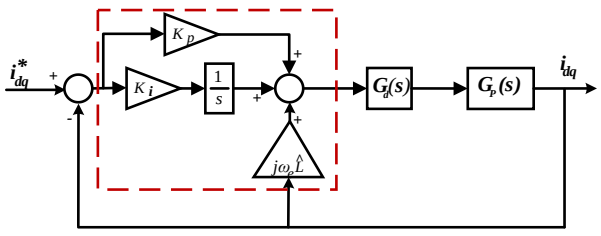

Fig. 2. Current control loop using conventional PI controller.

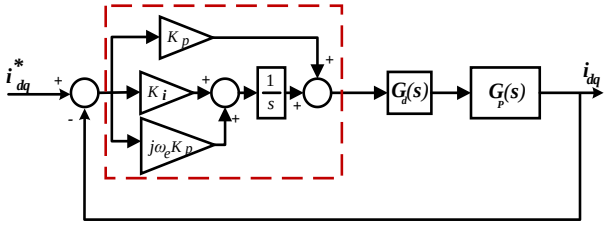

Fig. 3. Current control loop using complex vector PI controller.

$$G_{o.l.d}(s) = \frac{K_o}{s} G_d(s) \quad (5)$$

$$G_{c.l.d}(s) = \frac{K_o\, G_d(s)}{s + K_o\, G_d(s)} \quad (6)$$

Accordingly, the SRF PI CC can be tuned based on one parameter K_o that refers to the system bandwidth.

III. Active Disturbance Rejection Control

The current controller design based on ADRC is addressed in this section. The basic idea of the ADRC is to deal with the model uncertainties, un-modeled dynamics, and the external disturbances as a total disturbance which can be estimated in real-time by extended state observer (ESO). Then, an ESO-based feedback control that is used to compensate for the total disturbance and to keep the system output tracks the reference value [23]. Accordingly, a precise model of the system is not required. Moreover, it is simple to implement and has better disturbance rejection capability than other control techniques. The block diagram of the ADRC control scheme is shown in Fig. 4. Based on the ADRC principle [23, 24], it is assumed that the external disturbances and the process dynamics are represented as a total disturbance. Subsequently, the voltage equations of the PMSM model can be written such as:

$$\frac{di_d}{dt} = f_d + \frac{1}{L_d} u_d \quad (7)$$

$$\frac{di_q}{dt} = f_q + \frac{1}{L_q} u_q \quad (8)$$

$$f_d = -\frac{R_s}{L_d} i_d + \omega_e \frac{L_q}{L_d} i_q - \frac{1}{L_d} d_d \quad (9)$$

$$f_q = -\frac{R_s}{L_q} i_q - \omega_e \frac{L_d}{L_q} i_d - \frac{1}{L_q} \omega_e \phi_m - \frac{1}{L_q} d_q \quad (10)$$

where $i_{d,q}$, $u_{d,q}$, $L_{d,q}$, and $d_{d,q}$ correspond to dq axis stator current, voltages, inductances, and external disturbances respectively. R_s is the stator resistance and ϕ_m is the flux linkage of PMSM. Based on (7), the ESO can be expressed as follows: $u_o = v_q$, $b_o = 1/L_q$, and representing the q-axis by two states, $x_1 = i_q$ and $x_2 = f_q$. The total disturbance is represented by an extended state increasing the system order:

$$\begin{bmatrix} \dot{\tilde{x}}_1 \\ \dot{\tilde{x}}_2 \end{bmatrix} = \begin{bmatrix} 0 & 1 \\ 0 & 0 \end{bmatrix} \begin{bmatrix} \tilde{x}_1 \\ \tilde{x}_2 \end{bmatrix} + \begin{bmatrix} b_o' \\ 0 \end{bmatrix} u_o + \begin{bmatrix} l_1(y - \tilde{x}_1) \\ l_2(y - \tilde{x}_1) \end{bmatrix} \quad (11)$$

The observer gains can be determined based on the bandwidth parametrization method [25]. For the CC, the output feedback controller is designed based on the system

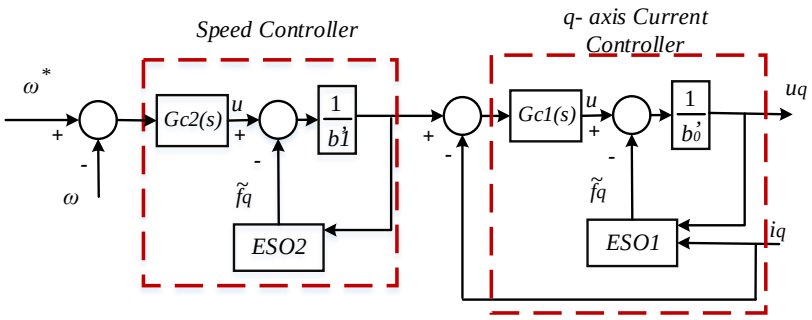

Fig. 4. Block diagram of the ADRC control scheme for current and speed loops.

output using the control law in (12):

$$u = K_{P1}(r - y) \tag{12}$$

where K_{P1} is the state feedback controller, r is the system input (the reference value of q-axis current), and u is the control signal generated from the feedback controller [26]. For the speed control loop based on ADRC, it can be designed as to (13):

$$\frac{d\omega_m}{dt} = -\frac{B}{J}\omega_m + \frac{1}{J}T_L + \frac{K_t}{J}i_q \tag{13}$$

where

$$K_t = 1.5\, p\phi_m$$

p is the pole pairs, T_L is the load torque, B is the friction coefficient and J represents the moment of inertia. Following the previous procedure with the current controller, ω_m will be the output y, i_q^* is the input u, and $b_o = \frac{K_t}{J}$.

IV. Model Predictive Control

MPC has been applied successfully for different applications to enhance the performance and robustness. It has been applied for different electrical machines including PMSM [27], [9]. MPC can replace the PI controllers' loops to obtain the FOC strategy taking into consideration the system constraints through the MPC cost function. To develop the MPC control loops, the PMSM state space needs to be identified. The differential equations of PMSM are given by [28]:

$$\frac{d}{dt}i_d = \frac{1}{L_d}(v_d - R_s\, i_d + L_q i_q\, \omega_e) \tag{14}$$

$$\frac{d}{dt}i_q = \frac{1}{L_q}(v_q - R_s\, i_q - L_d i_d\, \omega_e - \varphi_m \omega_e) \tag{15}$$

$$\frac{d}{dt}\omega_e = \frac{p}{J}(T_e - \frac{B}{p}\omega_e - T_L) \tag{16}$$

$$T_e = \frac{3p}{2}\,\varphi_m i_q \tag{17}$$

where T_e is the electromagnetic torque. The model given by (14) and (15) will be linearized around the operating point using Taylor expansion, and the linearized equations are:

$$I_q\omega_e = \omega_{e0}I_{q0} + I_{q0}(\omega_e - \omega_{e0}) + \omega_{e0}(I_q - I_{q0}) \tag{18}$$

$$I_d\,\omega_e = \omega_{e0}I_{d0} + I_{d0}(\omega_e - \omega_{e0}) + \omega_{e0}(I_d - I_{d0}) \tag{19}$$

where ω_{e0}, i_{d0} and i_{q0} are the operating point's values of the linearized model. By substituting (18) and (19) into (14) and (15), the linearized PMSM state-space model is derived as follows:

$$\dot{\mathbf{x}}(t) = \mathrm{A_m}\mathbf{x}(t) + \mathrm{B_m}\mathbf{u}(t) + \boldsymbol{\delta_m} \tag{20}$$

$$\boldsymbol{y}(t) = \mathrm{C_m}\mathbf{x}(t) + \mathrm{D_m}\mathbf{u}(t) \tag{21}$$

where

$$\mathbf{x}(t)^{\mathrm{T}} = [i_d \quad i_q \quad \omega_e]$$

$$\mathbf{u}(t)^{\mathrm{T}} = [v_d \quad v_q]$$

$$\mathbf{y}(t)^{\mathrm{T}} = [i_d \quad i_q \quad \omega_e]$$

$$\mathrm{A_m} = \begin{bmatrix} -\frac{R_s}{L_d} & \frac{L_q}{L_d}\omega_{e0} & \frac{L_q}{L_d}I_{q0} \\ -\frac{L_d}{L_q}\omega_{e0} & -\frac{R_s}{L_q} & -\left(\frac{L_d}{L_q}I_{d0} + \frac{\varphi_m}{L_q}\right) \\ 0 & \frac{3p^2\varphi_m}{2J} & -\frac{B}{J} \end{bmatrix}$$

$$\mathrm{B_m} = \begin{bmatrix} 1/L_d & 0 \\ 0 & 1/L_q \\ 0 & 0 \end{bmatrix},\ \boldsymbol{\delta_m} = \begin{bmatrix} -\frac{L_q}{L_d}\omega_{e0}I_{q0} \\ \frac{L_d}{L_q}\omega_{e0}I_{d0} \\ -\frac{pT_L}{J} \end{bmatrix}$$

$$\mathrm{C_m} = \begin{bmatrix} 1 & 0 & 0 \\ 0 & 1 & 0 \\ 0 & 0 & 1 \end{bmatrix},\ \mathrm{D_m} = 0$$

The model is discretized with a definite sampling time T_s using the forward Euler approximation method. The discretized state-space model of the system is:

$$\mathbf{x}(k+1) = \mathrm{A}\mathbf{x}(k) + \mathrm{B}\mathbf{u}(k) + \boldsymbol{\delta} \tag{22}$$

$$(k) = \mathrm{C}\mathbf{x}(k) + \mathrm{D}\mathbf{u}(k) \tag{23}$$

where

$$\mathrm{A} = \mathrm{I} + \mathrm{A_m}T_s =$$

$$\begin{bmatrix} T_s\left(1 - \frac{R_s}{L_d}\right) & T_s\omega_{e0} & T_sI_{q0} \\ -T_s\omega_{e0} & T_s(1 - \frac{R_s}{L_q}) & -T_s\left(I_{d0} + \frac{\varphi_m}{L_q}\right) \\ 0 & T_s(\frac{3p^2\varphi_m}{2J}) & T_s(1 - \frac{B}{J}) \end{bmatrix}$$

$$\mathrm{B} = \mathrm{B_m} T_s = \begin{bmatrix} {T_s}/{L_d} & 0 \\ 0 & {T_s}/{L_q} \\ 0 & 0 \end{bmatrix}$$

$$\boldsymbol{\delta} = \boldsymbol{\delta_m} T_s = \begin{bmatrix} -T_s \omega_{e0} I_{q0} \\ T_s \omega_{e0} I_{d0} \\ -T_s (\frac{p\, T_L}{J}) \end{bmatrix}$$

$$\mathrm{C} = \mathrm{C_m}, \mathrm{D} = \mathrm{D_m}$$

The MPC cost function is given by [27, 29]:

$$\boldsymbol{j} = \sum_{k=1}^{n_y} \mathbf{e}^{\mathbf{T}}(k) \mathrm{Q}(k)\, \mathbf{e}(k) + \sum_{k=0}^{n_u - 1} \mathbf{u}^{\mathbf{T}}(k) \mathrm{R}(k) \mathbf{u}(k) \quad (24)$$

subject to a discrete state-space model in (22) and (23), where $\mathbf{e}(k)_{3*1} = \mathbf{y}(k)_{3*1} - \mathbf{r}(k)_{3*1}$ is the error, $\mathbf{y}(k)_{3*1}$ is the system output, $\mathbf{r}(k)_{3*1}$ is the reference input**,** $\mathbf{u}(k)_{2*1}$ is the system control input, $\mathrm{Q}(k)_{3*3}$ and $\mathrm{R}(k)_{2*2}$ are weighting matrices, n_y is the prediction horizon value and n_u is the control horizon value. The model could be used recursively to find the predictions over the prediction horizon n_y as follows:

$$\hat{\mathbf{x}}(k+1) = \mathrm{P_x}\, \mathbf{x}(k) + \mathrm{H_x}\, \hat{\mathbf{u}}(k) \quad (25)$$

$$\hat{\mathbf{y}}(k+1) = \mathrm{P}\, \mathbf{x}(k) + \mathrm{H}\, \hat{\mathbf{u}}(k) \quad (26)$$

where

$$\hat{\mathbf{x}}(k+1) = \begin{bmatrix} \mathbf{x}(k+1) \\ \mathbf{x}(k+2) \\ \mathbf{x}(k+3) \\ \vdots \\ \mathbf{x}(k+n_y) \end{bmatrix}, \mathrm{P_x} = \begin{bmatrix} \mathrm{A} \\ \mathrm{A}^2 \\ \mathrm{A}^3 \\ \vdots \\ \mathrm{A}^{n_y} \end{bmatrix}$$

$$\mathrm{H_x} = \begin{bmatrix} \mathrm{B} & 0 & 0 & \dots \\ \mathrm{AB} & \mathrm{B} & 0 & \dots \\ \mathrm{A}^2\mathrm{B} & \mathrm{AB} & \mathrm{B} & \dots \\ \vdots & \vdots & \vdots & \vdots \\ \mathrm{A}^{n_y-1}\mathrm{B} & \mathrm{A}^{n_y-2}\mathrm{B} & \mathrm{A}^{n_y-3}\mathrm{B} & \dots \end{bmatrix}$$

$$\hat{\mathbf{u}}(k) = \begin{bmatrix} \mathbf{u}(k) \\ \mathbf{u}(k+1) \\ \mathbf{u}(k+2) \\ \vdots \\ \mathbf{u}(k+n_y-1) \end{bmatrix}, \hat{\mathbf{y}}(k+1) = \begin{bmatrix} \mathbf{y}(k+1) \\ \mathbf{y}(k+2) \\ \mathbf{y}(k+3) \\ \vdots \\ \mathbf{y}(k+n_y) \end{bmatrix}$$

$$\mathrm{P} = \begin{bmatrix} \mathrm{CA} \\ \mathrm{CA}^2 \\ \mathrm{CA}^3 \\ \vdots \\ \mathrm{CA}^{n_y} \end{bmatrix}, \mathrm{H} = \begin{bmatrix} \mathrm{CB} & 0 & 0 & \dots \\ \mathrm{CAB} & \mathrm{CB} & 0 & \dots \\ \mathrm{CA}^2\mathrm{B} & \mathrm{CAB} & \mathrm{CB} & \dots \\ \vdots & \vdots & \vdots & \vdots \\ \mathrm{CA}^{n_y-1}\mathrm{B} & \mathrm{CA}^{n_y-2}\mathrm{B} & \mathrm{CA}^{n_y-3}\mathrm{B} & \dots \end{bmatrix}$$

$\hat{\mathbf{x}}(k+1)_{(3*n_y)*1}$ is the predicted **s**ystem states, while $\hat{\mathbf{y}}(k+1)_{(3*n_y)*1}$ is the system output, $\hat{\mathbf{u}}(k)_{(2*n_y)*1}$ is the **s**ystem control input and $\mathrm{P}_{x(3*n_y)*3}$, $\mathrm{H}_{x(3*n_y)*(2*n_y)}$, $\mathrm{P}_{(3*n_y)*3}$, $\mathrm{H}_{(3*n_y)*(2*n_y)}$ are the system parameters, all over the prediction horizon n_y. The result of minimizing (24) with respect to $\mathbf{u}(k)$ is given by [30]:

TABLE I
PMSM PARAMETERS

Parameter	Symbol	Value
Rated Power	P	2300 W
Rated current	I_s	9.5 A
Rated Voltage	V_s	220 V
Rated Frequency	f	100 Hz
Stator resistance	R_s	0.55 Ω
Stator inductance	L_d, L_q	0.002225 H
Nominal Torque	T_m	15 Nm
Rotation speed	N_s	1500 RPM
Number of pole pairs	p	4
Stator-rotor flux	φ_m	0.114 wb
Rotor inertia	J	0.00277 kgm^2

$$\mathbf{u}(k)_{\mathbf{MPC}} = \mathrm{L}\big[(\mathrm{H}^{\mathrm{T}}\hat{\mathrm{Q}}(k)\mathrm{H} + \mathrm{H}^{\mathrm{T}}\hat{\mathrm{Q}}^{\mathrm{T}}(k)\mathrm{H} + 2\hat{\mathrm{R}}^{\mathrm{T}}(k))^{-1}\, 2\mathrm{H}^{\mathrm{T}}\hat{\mathrm{Q}}^{\mathrm{T}}(k)\big(\hat{\mathbf{r}}(k) - \mathrm{P}\mathbf{x}(k)\big)\big] \quad (27)$$

where $\mathrm{L}_{2*(2*n_y)} = [\mathrm{I}\ \ \mathrm{O}]$ with I_{2*2} is an identity matrix and $\mathrm{O}_{2*(2*\mathrm{ny}-2)}$ is a zero matrix, $\hat{\mathbf{r}}(k)_{(3*n_y)*1}$ is the reference input, $\hat{\mathrm{Q}}(k)_{(3*n_y)*(3*n_y)}$ and $\hat{\mathrm{R}}(k)_{(2*n_u-1)*(2*n_u-1)}$ are weighting matrices. One of the important features of MPC is solving the constrained optimization problem [31, 32]. There are many methods for handling system constraints, one of the simple approaches is softening constraints method, which has a low computation burden compared to the other approaches [33]. In this method, the system constraints are implemented as a sum of squares of the difference between the input constraints boundaries and system input in the cost function as follows:

$$\boldsymbol{j} = \sum_{k=1}^{n_y} \mathbf{e}^{\mathbf{T}}(k)\mathrm{Q}(k)\mathbf{e}(k) + \sum_{k=0}^{n_u-1} \mathbf{u}^{\mathbf{T}}(k)\mathrm{R}(k)\mathbf{u}(k) + \sum_{k=0}^{n_u-1} (\mathbf{u}(k) - \overline{\mathbf{u}}(k))^{\mathrm{T}}\, \mathrm{S}(k)\, (\mathbf{u}(k) - \overline{\mathbf{u}}(k)) \quad (28)$$

where $\overline{\mathbf{u}}(k)_{2*1}$ is the control input constraints boundaries and $\mathrm{S}(k)_{2*2}$ is the weighting matrix. Minimizing the cost function (28) with respect to $\mathbf{u}(k)$ will be:

$$\mathbf{u}(k)_{\mathbf{MPC}} = \mathrm{L}\Big[\Big(\mathrm{H}^{\mathrm{T}}\,\hat{\mathrm{Q}}(k)\mathrm{H} + \mathrm{H}^{\mathrm{T}}\,\hat{\mathrm{Q}}^{\mathrm{T}}(k)\mathrm{H} + 2\hat{\mathrm{R}}^{\mathrm{T}}(k) + 2\hat{\mathrm{S}}^{\mathrm{T}}(k)\Big)^{-1}\Big(2\mathrm{H}^{\mathrm{T}}\,\hat{\mathrm{Q}}^{\mathrm{T}}(k)\big(\hat{\mathbf{r}}(k) - \mathrm{P}\mathbf{x}(k)\big) + 2\hat{\mathrm{S}}^{\mathrm{T}}(k)\,\hat{\overline{\mathbf{u}}}(k)\Big)\Big] \quad (29)$$

where $\hat{\overline{\mathbf{u}}}(k)_{(2*n_u-1)*1}$ and $\hat{\mathrm{S}}(k)_{(2*n_u-1)*(2*n_u-1)}$ are the constraints values and weighting matrix over the control horizon $n_u - 1$ respectively.

V. Simulation Results

Simulations have been carried out using MATLAB/Simulink to test the addressed control schemes. The machine parameters are given in Table I. The control schemes are simulated by discrete-time blocks and the inverter is simulated by its average model. One step time delay is considered when the reference voltage is applied from the controller to the machine. The deadtime and the resistive voltage drop across diodes and transistors have been neglected. The switching frequency F_{sw} is decided to be 10 kHz. The control systems dynamics have been tested during a step-change in the mechanical load to test the speed of the response. The disturbance rejection capability for the external disturbances has been tested with an added

external disturbance to the output voltage in the q-axis, V_{dis} = 7 volts [34]. The system response for different control techniques at the nominal machine parameters is illustrated in Fig. 5. On the other hand, the machine resistance is increased by 10 % and the inductance is decreased by 5% in Fig. 6 to simulate the parameter variation effects on machine performance. Fig. 5 shows that the MPC scheme provides faster tracking for the step load changing followed by the ADRC scheme. However, it has an insignificant steady-state error with the d-axis current and speed. This error increases with the machine parameters mismatch as seen in Fig. 6.

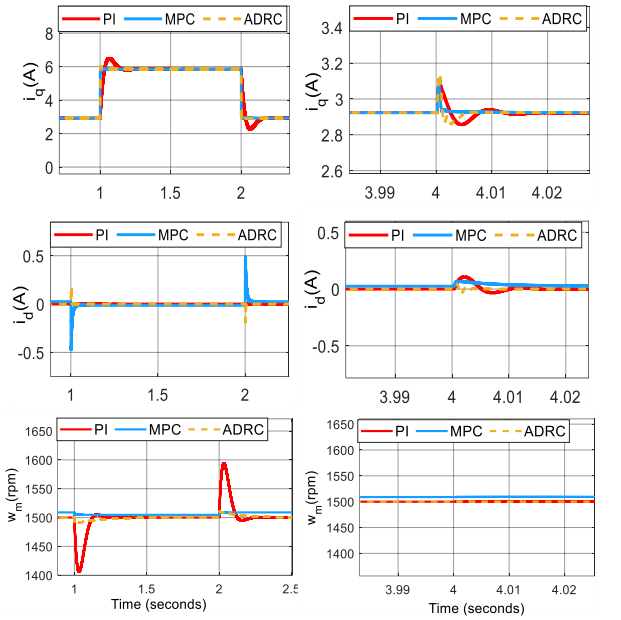

(a) Step loading change (b) External disturbance

Fig. 5. Current and speed responses during step loading change and external disturbance at nominal machine parameters.

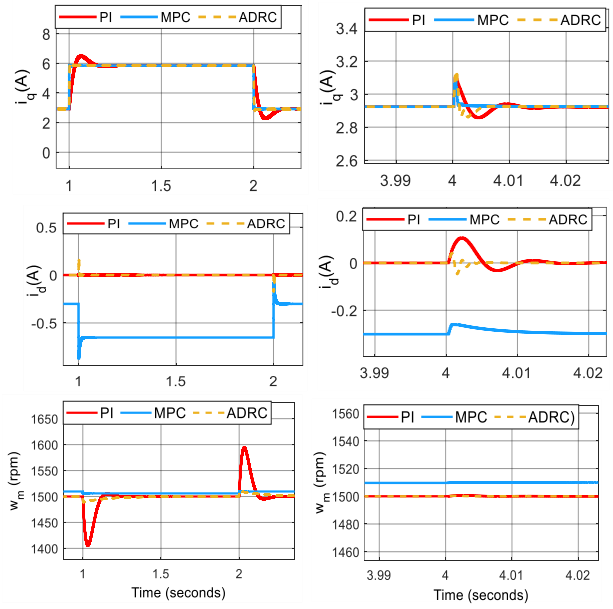

(a) Step loading change (b) External disturbance

Fig. 6. Current and speed responses during step loading change and external disturbance considering the machine parameter variations.

TABLE II
COMPARISON OF DIFFERENT CONTROL SCHEMES FOR AC DRIVES

Control Algorithm	Advantages	Disadvantages
PI Scheme	• Easy to implement and requires low memory. • Better cross-coupling compensation.	• Limited bandwidth due to system delays. • Machine parameters are required for proper tuning. • Low disturbance rejection capability.
ADRC Scheme	• High disturbance rejection capability. • The exact machine model is not required. • Easy to implement and requires low memory.	• The difficulty of tuning the controller gains. • Lack of providing perfect cross-coupling compensation.
MPC Scheme	• Fast dynamic behavior. • Lower harmonics distortion in motor currents.	• Sensitive to Machine parameters change. • Requires high computation burden.

For the ADRC scheme, it provides a better ability for disturbance rejection compared to other schemes. Moreover, it provides faster tracking for the load changes than the classical PI. However, it can be noticed that ADRC can not provide exact cross-coupling compensation compared to the PI scheme especially when the complex vector PI is used for current regulation. This issue is due to the lack of an observer to provide exact estimation and rejection. Another issue for the ADRC scheme is the tuning of the controller gains. It is still an interesting research area and needs more investigation.

VI. Conclusion

Three different control schemes including PI, ADRC, and MPC controllers have been studied for the PMSM motor drive. Their advantages and limitations have been summarized in Table II. It can be concluded that the MPC scheme has provided a faster dynamic performance and system delay ride through compared to PI and ADRC. However, it is sensitive to parameter variations and requires high mathematical computations. So, it is preferable for machines that have a limited change in their parameters and can be estimated by observers. For ADRC, it is simple to be implemented like the PI controller and it provides a higher disturbance rejection capability and faster dynamics. However, it takes some time to tune its parameters during the design process. Consequently, the proper tuning of the ADRC is still an open research area that need to be investigated.

References

[1] D. Gerada, A. Mebarki, N. L. Brown, C. Gerada, A. Cavagnino, and A. Boglietti, "High-Speed Electrical Machines: Technologies, Trends, and Developments," *IEEE*

Transactions on Industrial Electronics, vol. 61, no. 6, pp. 2946-2959, 2014.

[2] M. Galea, P. Giangrande, V. Madonna, and G. Buticchi, "Reliability-Oriented Design of Electrical Machines: The Design Process for Machines' Insulation Systems MUST Evolve," *IEEE Industrial Electronics Magazine*, vol. 14, no. 1, pp. 20-28, 2020.

[3] P. Giangrande, V. Madonna, S. Nuzzo, and M. Galea, "Moving Toward a Reliability-Oriented Design Approach of Low-Voltage Electrical Machines by Including Insulation Thermal Aging Considerations," *IEEE Transactions on Transportation Electrification*, vol. 6, no. 1, pp. 16-27, 2020.

[4] F. Briz and M. Hinkkanen, "Design, implementation and performance of synchronous current regulators for AC drives," *Chinese Journal of Electrical Engineering*, vol. 4, no. 3, pp. 53-65, 2018.

[5] P. Giangrande *et al.*, "Considerations on the Development of an Electric Drive for a Secondary Flight Control Electromechanical Actuator," *IEEE Transactions on Industry Applications*, vol. 55, no. 4, pp. 3544-3554, 2019.

[6] D. G. Holmes, T. A. Lipo, B. P. McGrath, and W. Y. Kong, "Optimized Design of Stationary Frame Three Phase AC Current Regulators," *IEEE Transactions on Power Electronics*, vol. 24, no. 11, pp. 2417-2426, 2009.

[7] S. Li, B. Sarlioglu, S. Jurkovic, N. R. Patel, and P. Savagian, "Analysis of Temperature Effects on Performance of Interior Permanent Magnet Machines for High Variable Temperature Applications," *IEEE Transactions on Industry Applications*, vol. 53, no. 5, pp. 4923-4933, 2017.

[8] A. Diab, M. Rashed, J. Li, C. Gerada, and S. Bozhko, "Performance Analysis of PMSM for High-Speed Starter-Generator System," in *2018 IEEE International Conference on Electrical Systems for Aircraft, Railway, Ship Propulsion and Road Vehicles & International Transportation Electrification Conference (ESARS-ITEC)*, 2018, pp. 1-7.

[9] S. S. Yeoh, T. Yang, L. Tarisciotti, C. I. Hill, S. Bozhko, and P. Zanchetta, "Permanent-Magnet Machine-Based Starter–Generator System With Modulated Model Predictive Control," *IEEE Transactions on Transportation Electrification*, vol. 3, no. 4, pp. 878-890, 2017.

[10] M. Hyung-Tae, K. Hyun-Soo, and Y. Myung-Joong, "A discrete-time predictive current control for PMSM," *IEEE Transactions on Power Electronics*, vol. 18, no. 1, pp. 464-472, 2003.

[11] X. Chang, Y. Li, W. Zhang, N. Wang, and W. Xue, "Active Disturbance Rejection Control for a Flywheel Energy Storage System," *IEEE Transactions on Industrial Electronics*, vol. 62, no. 2, pp. 991-1001, 2015.

[12] J. Yang, H. Cui, S. Li, and A. Zolotas, "Optimized Active Disturbance Rejection Control for DC-DC Buck Converters With Uncertainties Using a Reduced-Order GPI Observer," *IEEE Transactions on Circuits and Systems I: Regular Papers*, vol. 65, no. 2, pp. 832-841, 2018.

[13] S. Bosheng and G. Zhiqiang, "A DSP-based active disturbance rejection control design for a 1-kW H-bridge DC-DC power converter," *IEEE Transactions on Industrial Electronics*, vol. 52, no. 5, pp. 1271-1277, 2005.

[14] S. Li, C. Xia, and X. Zhou, "Disturbance rejection control method for permanent magnet synchronous motor speed-regulation system," *Mechatronics*, vol. 22, no. 6, pp. 706-714, 2012/09/01/ 2012.

[15] Y. Zhao and L. Dong, "Robust current and speed control of a permanent magnet synchronous motor using SMC and ADRC," *Control Theory and Technology*, journal article vol. 17, no. 2, pp. 190-199, May 01 2019.

[16] B. Guo, S. Bacha, and M. Alamir, "A review on ADRC based PMSM control designs," in *IECON 2017 - 43rd Annual Conference of the IEEE Industrial Electronics Society*, 2017, pp. 1747-1753.

[17] F. Guo, T. Yang, S. Bozhko, and P. Wheeler, "A Novel Virtual Space Vector Modulation Scheme for Three-Level NPC Power Converter with Neutral-Point Voltage Balancing and Common-Mode Voltage Reduction for Electric Starter/Generator System in More-Electric-Aircraft," in *2019 IEEE Energy Conversion Congress and Exposition (ECCE)*, 2019, pp. 1852-1858.

[18] Z. Huang, T. Yang, P. Giangrande, S. Chowdhury, M. Galea, and P. Wheeler, "An Active Modulation Scheme to Boost Voltage Utilization of the Dual Converter With a Floating Bridge," *IEEE Transactions on Industrial Electronics*, vol. 66, no. 7, pp. 5623-5633, 2019.

[19] M. Kadjoudj, M. E. H. Benbouzid, C. Ghennai, and D. Diallo, "A robust hybrid current control for permanent-magnet synchronous motor drive," *IEEE Transactions on Energy Conversion*, vol. 19, no. 1, pp. 109-115, 2004.

[20] A. G. Yepes, A. Vidal, J. Malvar, O. López, and J. Doval-Gandoy, "Tuning Method Aimed at Optimized Settling Time and Overshoot for Synchronous Proportional-Integral Current Control in Electric Machines," *IEEE Transactions on Power Electronics*, vol. 29, no. 6, pp. 3041-3054, 2014.

[21] F. Briz, M. W. Degner, and R. D. Lorenz, "Analysis and design of current regulators using complex vectors," *IEEE Transactions on Industry Applications*, vol. 36, no. 3, pp. 817-825, 2000.

[22] J. Holtz, Q. Juntao, J. Pontt, J. Rodriguez, P. Newman, and H. Miranda, "Design of fast and robust current regulators for high-power drives based on complex state variables," *IEEE Transactions on Industry Applications*, vol. 40, no. 5, pp. 1388-1397, 2004.

[23] J. Han, "From PID to Active Disturbance Rejection Control," *IEEE Transactions on Industrial Electronics*, vol. 56, no. 3, pp. 900-906, 2009.

[24] A. M. Diab, S. Bozhko, M. Galea, and C. Gerada, "Stable and Robust Design of Active Disturbance Rejection Current Controller for Permanent Magnet Machines in Transportation Systems," *IEEE Transactions on Transportation Electrification*, pp. 1-1, 2020.

[25] G. Zhiqiang, "Scaling and bandwidth-parameterization based controller tuning," in *Proceedings of the 2003 American Control Conference, 2003.*, 2003, vol. 6, pp. 4989-4996.

[26] M. F. Golnaraghi, *Automatic control systems*, 9th ed. / Farid Golnaraghi, Benjamin C. Kuo. ed. Hoboken, N.J.: Hoboken, N.J. : Wiley, 2010.

[27] A. A. Abdelrauf, W. W. Saad, A. Hebala, and M. Galea, "Model Predictive Control Based PID Controller for PMSM for Propulsion Systems," in *2018 IEEE International Conference on Electrical Systems for Aircraft, Railway, Ship Propulsion and Road Vehicles & International Transportation Electrification Conference (ESARS-ITEC)*, 2018, pp. 1-7.

[28] S. Chai, L. Wang, and E. Rogers, "Model predictive control of a permanent magnet synchronous motor with experimental validation," *Control Engineering Practice*, vol. 21, no. 11, pp. 1584-1593, 2013/11/01/ 2013.

[29] A. A. Abdelrauf, M. Abdel-Geliel, and E. Zakzouk, "Adaptive PID controller based on model predictive control," in *2016 European Control Conference (ECC)*, 2016, pp. 746-751.

[30] A. Aboelhassan, "Design and Implementation of an Industrial Controller Using Advanced Automation Technology," MSc Thesis, Electrical and Control Engineering Department, AASTMT, 2016.

[31] B. Zhu, Z. Zheng, and X. Xia, "Constrained Adaptive Model-Predictive Control for a Class of Discrete-Time Linear Systems With Parametric Uncertainties," *IEEE Transactions on Automatic Control*, vol. 65, no. 5, pp. 2223-2229, 2020.

[32] T. Tarczewski and L. M. Grzesiak, "Constrained State Feedback Speed Control of PMSM Based on Model Predictive Approach," *IEEE Transactions on Industrial Electronics*, vol. 63, no. 6, pp. 3867-3875, 2016.

[33] J. M. Maciejowski, *Predictive Control: With Constraints*. Prentice Hall, 2002.

[34] Y. Liao, F. Li, H. Lin, and J. Zhang, "Discrete current control with improved disturbance rejection for surface-mounted permanent magnet synchronous machine at high speed," *IET Electric Power Applications*, vol. 11, no. 7, pp. 1333-1340, 2017.